Fermi National Accelerator Laboratory

FERMILAB-Conf-99/105-E
CDF

W, Z + Jets at Tevatron

Paoti Chang
For the CDF Collaboration

Institute of Physics, Academia Sinica
Academy Rd., Sec 2, Nankang, Taipei, Taiwan, ROC

Fermi National Accelerator Laboratory
P.O. Box 500, Batavia, Illinois 60510

April 1999

Published Proceedings of the *13th Topical Conference on Hadron Collider Physics*,
Mumbai, India, January 14-20, 1999

Operated by Universities Research Association Inc. under Contract No. DE-AC02-76CH03000 with the United States Department of Energy

W,Z + JETS AT TEVATRON

PAOTI CHANG
Institute of Physics, Academia Sinica,
Academy Rd., Sec 2, Nankang, Taipei, Taiwan, ROC
E-mail: pchang@sinica.edu.tw

We report the production jet cross-sections and properties in W and Z events using data from collisions with $\sqrt{s} = 1800$ GeV at Fermilab Tevatron. Observed distributions in general agree with predictions of leading order QCD matrix element calculations with added gluon radiations and simulated parton fragmentations; however, some limitations of LO QCD predictions are also observed. The cross-section ratio of W $+ \geq 1$ jet events to inclusive W events is reported and compared with next-to-the-leading order QCD expectations. Good agreement between data and theory is seen. The color coherence effects are also observed in $W+$ jets events.

1 Motivation

A relatively large sample of W and Z events has been collected from both CDF and D0 experiments during 1992-1996 Tevatron run. These data are large enough to study the hadronic properties of high energy jets associated with W, Z boson production. These $p\bar{p} \to W, Z$ + jets events provide a good test of Quantum Chromodynamics (QCD) because the event sample has small ground and the presence of W, Z bosons select high Q^2 events. Besides, $W, Z+$ jets events are the background of top quark, Higgs, and SUSY productions. One needs to understand the background in order to serach for signals. Therefore, the study of W, Z production properties becomes essential.

2 Z + jets

CDF has studied the jet properties in Z events using the electron sample. The trigger electrons identified by the central calorimeter and tracking system are required to be isolated, have transverse energy $E_T > 20$ GeV and situate at pseudorapidity $|\eta| < 1.1$. And then we search for the second electron in the calorimeter upto $|\eta| < 3.7$. Jets are identified using cone algorithem with $\Delta R < 0.4$ and the corresponding energies are corrected to account for calorimeter response, fragmentation energies outside the cone, and underlying energies in the jets. Jets are required to have $E_T > 15$ GeV, $|\eta| < 2.4$ and jet-jet separation $\Delta R_{jj} > 0.52$. If the separation of two jets is less than 0.52, these two jets are merged into one jet. A event sample of 6708 $Z \to e^+e^-$ decays is selected by requiring the electron pair masses to be within 15 GeV/c^2 of the nominal Z boson mass.

The Z boson background are dominated by jets faking electrons, which are estimated using data. Besides, there are small background of $Z+$ jets events from $W \to e\nu+$ jet, $Z \to \tau^+\tau^-$ and $Z+$ photon events, which are estimated from Monte carlo simulations. The detailed description of this analysis can be found in Ref.[1].

Figure 1 shows Z production cross-section times branching ratio of $Z \to e^+e^-$ as a function of jet multiplicity. Also show in the figure is the QCD preictions obtained

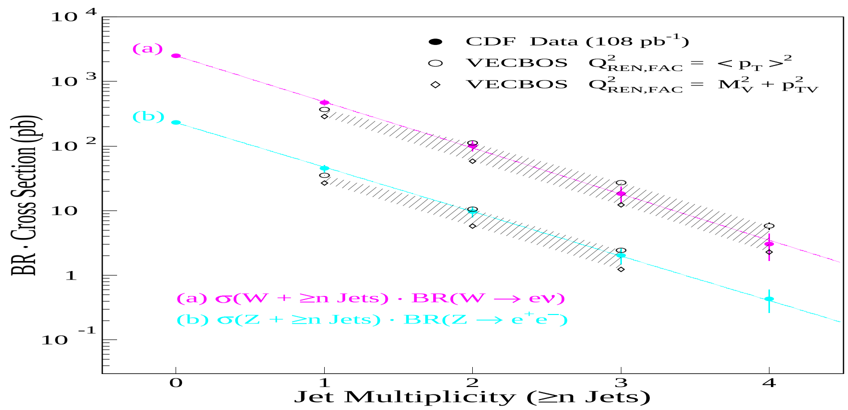

Figure 1. The W,Z + jets cross-sections as a function of jet multiplicity.

from leading order parton level calculation (VECBOS[2]) plus gluon radiations and parton fragmentations using the HERWIG[3] shower simulation algorithem. Two renormailzation scales, $Q^2 = \langle P_T \rangle^2$ and $Q^2 = M_T^2 + P_{T_Z}^2$, and two parton distribution functions, MRSA and CTEQ3M, are used in obtaining predictions. For $Q^2 = \langle P_T \rangle^2$, the measured $Z+ \geq n$ jet cross sections range from 0.83 to 1.29 times the QCD predictions, while for $Q^2 = M_T^2 + P_{T_Z}^2$, the cross sections are larger than the predictions by nearly constant at 1.7. The QCD predictions are indistinguishable for the two parton distribution functions within the statistical uncertainties.

The jet E_T spectra of first, second, and third highest E_T jets are consistent with the modified LO QCD expectations. And we also find that LO QCD also describes well the jet-jet separation (ΔR_{jj}) distributions in $\eta - \phi$ space and the $\cos\theta^*$ distributions where θ^* is the angle between the Z boson and the average beam directions in the Z + leading jet center-of-mass frame (see Ref.[1]).

The other interesting information is the number of jets with secondary vertices which are characteristic of b jets. Among 1665 jets in this Z sample, six secondary vertex candidates are found and 6.3 ± 1.0 events are expected from the inclusive jet data sample, indicating that there are no more b quarks associated with Z production above the expectation.

3 W + jets

The jet properties of W ($W \rightarrow e\nu$) events are also reported by the CDF collaboration using the inclusive electron data. The same method described in the previous section is employed to select the trigger electrons and jets. A missing transverse energy cut , $\not\!\!E_T > 30$ GeV, is applied to identify neutrinos. Using 108 pb^{-1} data, 51341 W candidates are observed. The main W + jets background comes from the multijet events where one jet fakes an electron and the misreconstruction of jets mimics a large missing E_T. This background as a function of jet multiplicity is estimated from data. The other backgrounds such as $Z \to e^+e^-$, $W \to \tau\nu$, di-boson, and $t\bar{t}$ production are estimated using Monte Carlo data. The more detailed description of this analysis can be found in Ref.[4].

Figure 1 shows the W cross-sections times $W \to e\nu$ branching ratio as a function of jet multiplicity. The W production cross-section is around an order of magnitude larger than the Z cross-section. The number of W events, as in the Z case, drops to a factor of $\frac{1}{5}$ with an additional jet requirement. From this rate, we expect to observe $W + 6$ jets events in Tevatron Run II. The QCD expectations are obtained using the same method described in the $Z+$ jets analysis. Data is around 60% larger than QCD predictions for the hard scale ($Q^2 = M_w^2 + P_{TW}^2$), and from around 28% larger than the prediction for $W + 1$ jet to around half of the prediction for $W + 4$ jets using the soft scale ($Q^2 = \langle P_T \rangle^2$). Therefore, within the inherent uncertainty of LO QCD calculations, the predicted and measured $W + n$ jets cross-sections are in agreement for $n = 2$ to 4.

Details of jet properties are studied using kinematic distributions of jets in W events. Fig. 2 shows the transverse energy distributions for first, scond, third, and fourth highest E_T jets. The corresponding LO QCD predictions are also shown in the figure using two different renormalization scales. The more detailed comparison can be clearily seen in Fig. 3. The theoretical QCD calculations underestimate the cross-section for lowest E_T ($E_T < 20$ GeV) and highest E_T ($E_T > 100$ GeV) jets. At low E_T, the initial state gluon radiation is sometimes hard enough to become the highest E_T jet, which is not fully predicted by the HERWIG model. For events with jet $E_T > 100$ GeV, over 50% of the $W+ \geq 1$ jet events have at least two

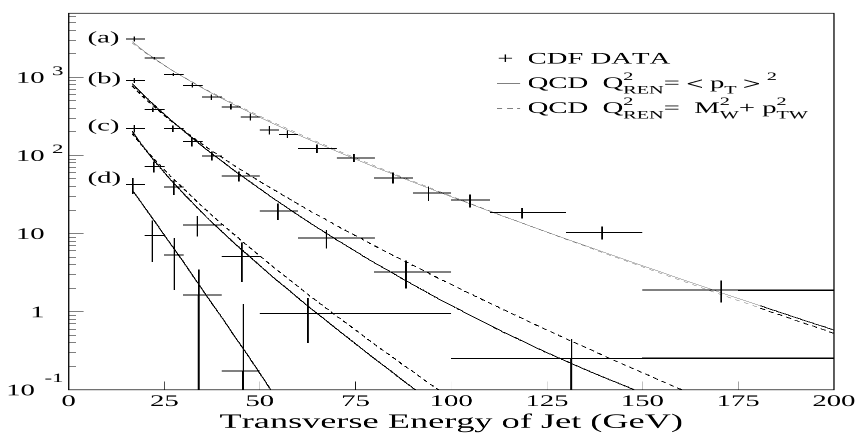

Figure 2. The transverse energy distributions of the (a) highest E_T jet in $W+ \geq 1$ jet events, (b) second highest E_T jet in ≥ 2 jets events, (c) third highest E_T jet in ≥ 3 jets events, and (d) fourth highest E_T jet in ≥ 4 jet events. The solid curve shows the LO QCD predictions (VECBOS+HERWIG) with $Q^2 = \langle P_T \rangle^2$, while the dashed curves with $Q^2 = M_w^2 + P_{TW}^2$. The theory is normailzed to data and the errors are the sum of statistical and systematic uncertainties.

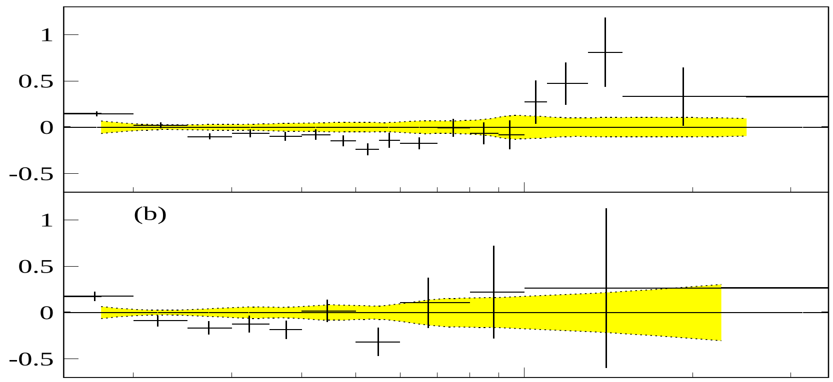

Figure 3. (Data-theory)/theory ($Q^2 = \langle P_T \rangle^2$) for the jet transverse energy distribution of the (a) first and (b) second highest E_T jets. The error bars are statistical uncertainties and the band represents the systematic uncertainties.

jets which is not expected from LO QCD calculations and indicates the need for higher order corrections. The observed jet-jet separation (ΔR_{jj}) and di-jet mass distribution (M_{jj}) are found to be in agreement with the QCD predictions (see Ref.[4]).

4 $\mathbf{R}_{10}$ measurement

Another interesting variable to study the jet properties is the ratio (R_{10}) of $W+\geq 1$ jet cross-section to inclusive W cross-section. Since the next to the leading order QCD calculation is available for $W+1$ jet events, this R_{10} study provides futher test of QCD with less theoretical uncertainty caused by the renormalization scale. Besides, the uncertainty of integrated luminosity gets cancelled and lots of systematic uncertainties are reduced in measuring the cross-section ratio.

CDF collaboration has compared this measured R_{10} value as a function of minimum jet E_T (E_T^{min}) requirement with QCD prediction. The same method as described in the previous section is used to select W events. In addition to identify jets using the cone size 0.4, cone size 0.7 is also adopted to provide futher comparisons. Unlike the previous $W, Z+$ jets analyses, no jet merging is performed and this merging effect is actually very small. All the $W+$ jets background are studied using both data and Monte Carlo simulations, and the corresponding corrections[5] are measured for each E_T^{min}. The acceptance for $W \to e\nu$ events, which corrects for losses due to fiducial and kinematic requirements on both electrons and $\not{E}_T$ is determined from Monte Carlo plus detector simulations. The electron trigger and identification efficiency and electron-jet overlap efficiency are all measured from data[5]. The theoretical QCD predictions are obtained by using the DYRAD[6] Monte Carlo program, which calculates the NLO QCD matrix elements in the parton level.

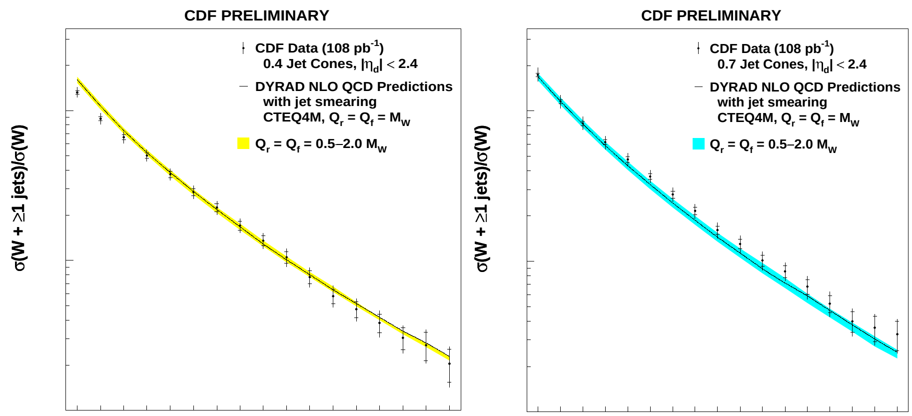

Figure 4. R_10 values as a function of jet E_T^{min} for 0.4 jet cones(left) and 0.7 jet cones(right). The curves are NLO QCD predictions using CTEQ4M parton distribution functions with bands characterizing the uncertainties from using different scales.

The parton energy is then smeared according to the jet energy uncertainty we understand in data. Parton-parton separation is required to be 1.3 times the jet cone size.

Figure 4 shows the R_{10} value as a function of E_T^{min} using both 0.4 and 0.7 cone size jets. Superimposed in the plot is the NLO QCD predictions with bands indicating the uncertainties using different renormalization (Q_r) and factorization (Q_f) scales. In general, NLO QCD describes data very well: within 15% for 0.4 cone size jets and 20% for 0.7 cones. For $E_T^{min} < 25$ GeV, QCD predictions are larger than data for 0.4 jet cone case, suggesting that the soft gluon effects, which are not included in the DYRAD calculation, may be large in the low E_T region. Since jets with larger cone sizes cover more soft gluons, this gluon radiation effect is less severe in 0.7 jet cone case. The difference of NLO QCD calculations due to different parton distribution functions has been studied using CTEQ4M and MRSA'; no substantial differences is found.

A comparison with NLO QCD and LO QCD calculations (also from DYRAD) has been made and the effect can be clearly seen in Fig. 5, where $[R_{10}(data) - R_{10}(NLOQCD)]/R_{10}(NLOQCD)$ is ploted with the superimposition of $[R_{10}(LOQCD) - R_{10}(NLOQCD)]/R_{10}(NLOQCD)$ using CTEQ4M PDF's and the renormalization (Q_r) and factorization (Q_f) scales ranging from $0.5M_W$ to $2.0M_W$. Varying both scales together by a factor of two results in a 5% change at NLO QCD but 15% change at LO QCD. The LO and NLO predictions differ by less than 11%.

The predicted R_{10} due to different $\alpha_s(M_z)$ values (with different corresponding PDF's) has also been studied and the preictions show very little sensitivity to variations to α_s. Fig. 6 shows a plot of R_{10} vs $\alpha_s(M_z)$ for various PDF sets in the MRSA and CTEQ4 families. Data and QCD predictions agree in all α_s values.

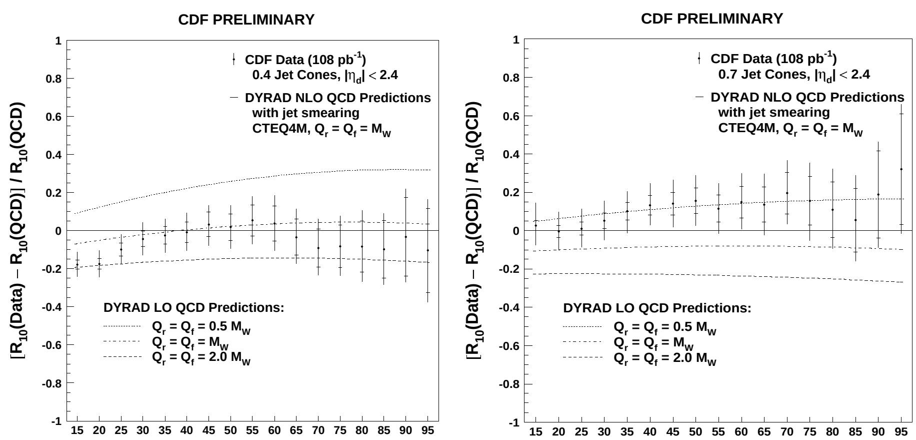

Figure 5. $R_{10}(data) - R_{10}(NLOQCD)/R_{10}(NLOQCD)$ as a function of jet E_T^{min}. Superimposed is $R_{10}(LOQCD) - R_{10}(NLOQCD)/R_{10}(NLOQCD)$ with different scales.

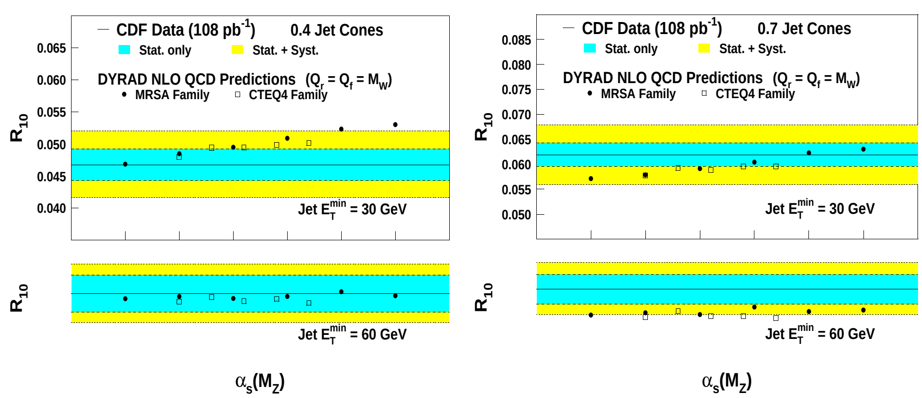

Figure 6. R_{10} vs $\alpha_s(M_z)$. The measured R_{10} values with statistical and systematic uncertainties for $E_T^{min} = 30$ GeV and $E_T^{min} = 60$ GeV are represented by horizontal bars.

5 Color coherence in W + jets events

Color coherence phenomena were first observed in $e^+ - e^-$ experiments[7] in the 80's. What people observed was that the particle production in the region between quark and anti-quark jets in $e^+e^- \rightarrow q\bar{q}g$ events was suppressed. In PQCD, such effects arise from the destructive intereference of soft gluons radiated from q, $\bar{q}$, and g. An alternative explanation is that color-connected partons act like color antennae.

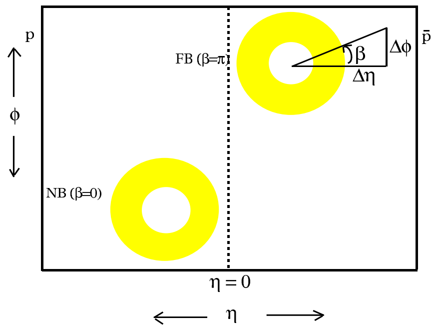

Figure 7. Calorimeter view in $\eta - \phi$ space. The center of two inner circles respresent the W and jet directions. Two annuli are defined in the band region ($0.7 < \Delta R < 1.5$). Calorimeter towers inside the band region are used in the analysis.

Particles are radiated from the color connected line; therefore, particle production is suppressed in the region between q and $\bar{q}$, in which no color line is connected.

D0 collaboration has explored the initial-to-final state coherence effects in $W+$ jets events by comparing the soft particle flows in the jet side (color connected) and that in the W side (colorless). $W \to e\nu$ candidates are selected from events satisfying D0 online triggers by requiring $\not\!\!E_T > 25$ GeV and high quality electrons with $E_T > 25$ GeV. Jets are identified using the cone algorithem with cone size of 0.7. W candidates are required with rapidity $\mid y \mid < 0.7$ and the highest E_T jet in an event is required to be central in pseudo-rapidity ($\mid \eta \mid < 0.7$) and in the opposite ϕ hemisphere ($\pi/2 < \Delta\phi < 3\pi/2$) of W. Annuli are defined in the W and jet directions (see Fig.7) and the number of calorimeter towers N with $E_T > 250$ MeV is measured as a function of β ($\tan^{-1}(sign(\eta_{W,jet})\Delta\phi/\Delta\eta)$. To improve statistics, annuli are folded about ϕ axis; consequently β ranges from 0 to π. Color coherence effects are expected to produce larger multiplicities around $\beta = 0$ (near beam) and $\beta = \pi$ (far beam) regions in the jet side and particles are more or less uniformly distributed in the W side. Measuring N_{jet}/N_W as a function of β tests this prediction and the ratio method reduces the sensitivity to global detector and underlying event biases.

Observed N_{jet}/N_W distributions are compared with QCD predictions using PYTHIA[8] generator plus full detector simulation. Color coherence effects in PYTHIA are implemented using angular ordering (perturbative) and string fragmentation (non-perturbative), which can be turned on and off independently. In addition, analytic PQCD predictions by Khoze and Stirling[9] are also used for comparisons. Fig. 8 shows the comparisons. The agreement between data and both PYTHIA with color coherence effects on and analytic QCD predictions supports the observation of coherence effects in W data.

6 Summary

Jet properties in W events have been compared to QCD expectations in several analyses. Good agreement between data and LO QCD predictions in $W, Z + n$ jets

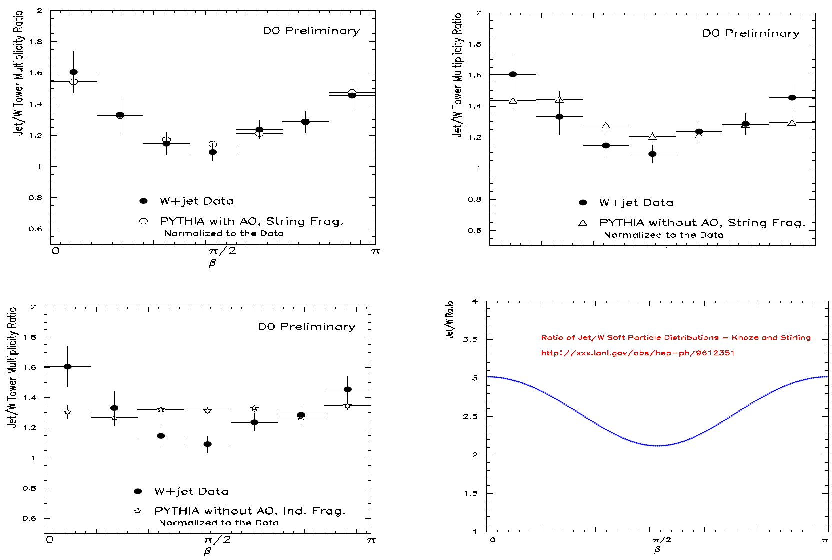

Figure 8. Tower multiplicity ratio vs β for W data in comparing to PYTHIA QCD predictions with three different implementations of angular ordering and fragmenation, and to analytical QCD predictions (bottom right).

cross sections and jet properties is observed by CDF although some limitations of LO QCD calcuations are found in W data. The R_{10} distributions are well described by NLO QCD predictions according to CDF analyses. D0 has studied the color coherence effects using $W+$ jets data and the initial-to-final state coherence effects are confirmed.

References

1. F. Abe *et al.*, the CDF collaboration, Phys. Rev. Lett. 77, 448 (1996).
2. F.A. Berends, W.T. Giele, H. Kuijf, and B. Tausk, Nucll. Phys. B 357, 32 (1991).
3. G. Marchesini *et al.*, comput. Phys. Comm. 67, 465 (1992).
4. F. Abe *et al.*, the CDF collaboration, Phys. Rev. Lett. 79, 4760 (1997)
5. F. Abe *et al.*, The CDF Collaboration, Phys. Rev. Lett. 81, 1367 (1998).
6. W.T. Giele, E.W.N. Glover, and D.A. Kosower, Nucl. Phys. B403, 633 (1993).
7. H. Aihara *et al.*, TPC/2γ Collaboration, Phys. Rev. Lett. 54, 270(1985) P.D. Sheldon *et al.*, MARK2 Collaborations, Phys. Rev. Lett. 57, 1398(1986); M.Z. Akrawy *et al.*, OPAL Collaboration, Phys. Lett. B247, 617 (1990).
8. T. Sjöstrand, Comput. Phys. Commun. 82, 74(1994).
9. V.A. Khoze and J. Stiring, Zeit. Phys. C76, 59(1997).